

**Electronic supporting information (ESI)**

**Superior gravimetric CO<sub>2</sub> uptake of aqueous deep-eutectic solvent solutions**

Shashi Kant Shukla<sup>\*a</sup>, Yong-Lei Wang<sup>a</sup>, Aatto Laaksonen<sup>b</sup>, Xiaoyan Ji<sup>\*a</sup>

<sup>a</sup>Energy Engineering, Division of Energy Science, Luleå University of Technology, 97187

Luleå, Sweden

<sup>b</sup>Energy Engineering, Division of Energy Science, Luleå University of Technology, 97187 Luleå

Sweden; Division of Physical Chemistry, Department of Materials and Environmental

Chemistry, Arrhenius Laboratory, Stockholm University, Stockholm 10691, Sweden; Center of

Advanced Research in Bionanoconjugates and Biopolymers, “Petru Poni” Institute of

Macromolecular Chemistry, Iasi 700469, Romania; State Key Laboratory of Materials Oriented

and Chemical Engineering, Nanjing Tech University, Nanjing 211816, China

Emails: [Shashi.kant.shukla@associated.ltu.se](mailto:Shashi.kant.shukla@associated.ltu.se), [Xiaoyan.ji@ltu.se](mailto:Xiaoyan.ji@ltu.se)

## 1. Synthesis of DESs

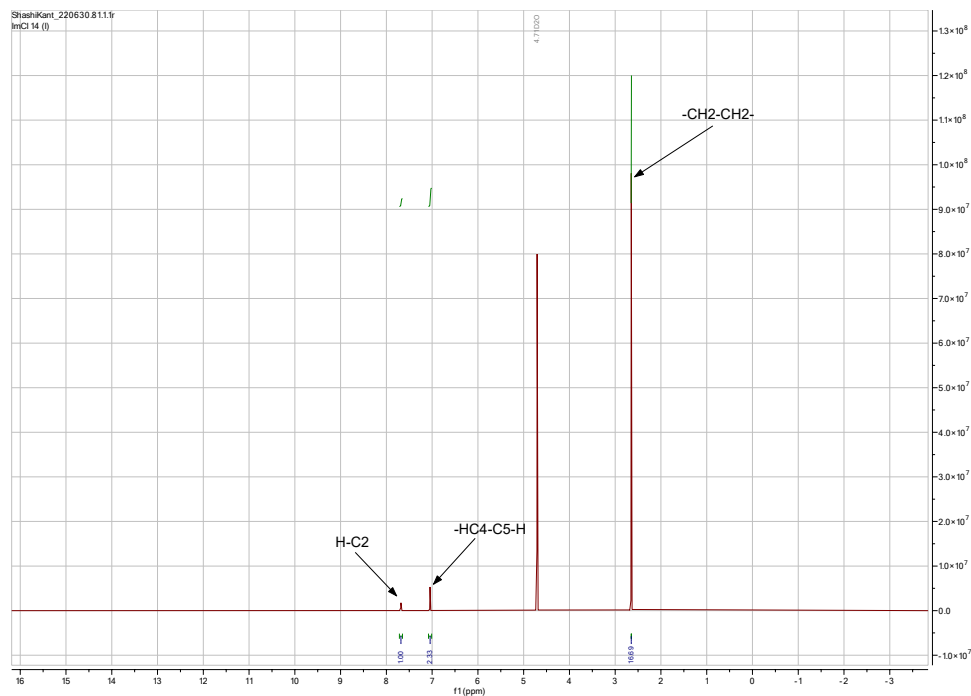
Imidazolium ([Im])-based DESs were prepared in two steps. The first step involved the protonation of imidazolium by the dropwise addition of hydrochloric acid under vigorous stirring at 0 °C in a 1:1 mole ratio for 6h. The resultant protic ionic liquid (PIL) was subjected to a rotary evaporator under reduced pressure to get rid of excess water. The dried PIL was further subjected to an ultra-vacuum at 60 °C for 6h to remove traces of water vapor and other volatile impurities. The synthesized PIL is used as a hydrogen bond acceptor (HBA). The second step involved the complexation of the PIL with hydrogen bond donor (HBD) ethylenediamine (EDA) at 1:4, 1:5, and 1:6 molar ratios at 70 °C for 6 hours to get the desired DESs. The synthesized DESs were characterized by the <sup>1</sup>H- and <sup>13</sup>C-NMR spectroscopic methods (see entry 2). The water content of the resulting DESs, as measured by the Karl-Fisher Coulometer, were below 40 ppm before the experiment. The thermal stability of the synthesized DESs as obtained by the thermogravimetric analysis (TGA) was between 200 – 225°C.

## 2. Characterization of DESs

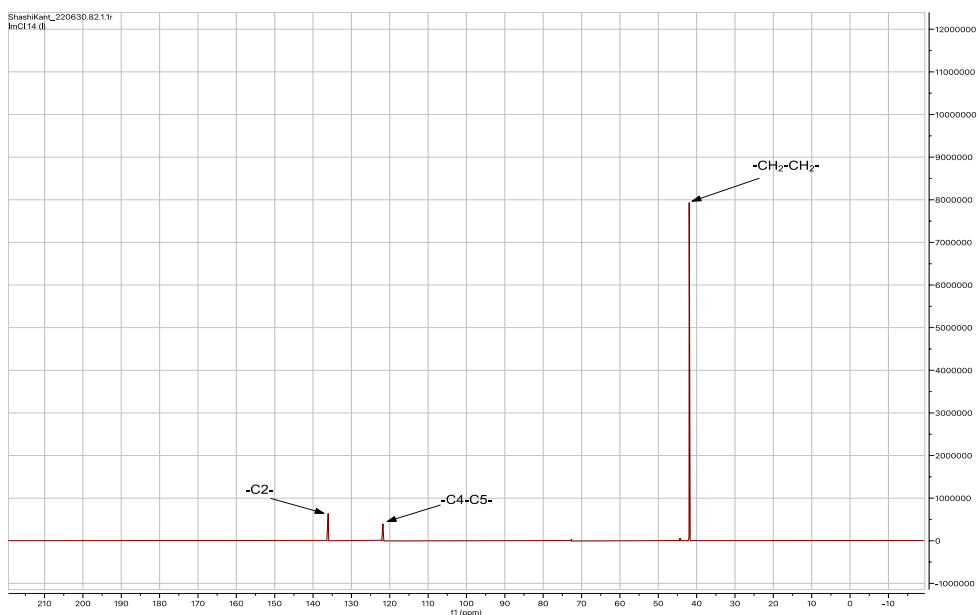
[Im.Cl][EDA]=1:4

a)  $^1\text{H}$  NMR (400 MHz,  $\text{D}_2\text{O}$ , 25 °C):  $\delta\text{H}$  (ppm): 2.67 (s,  $\text{CH}_2\text{-NH}_2$  of EDA), 7.0 (s,  $\text{H-C}_4\text{-C}_5\text{-H}$ ), and 7.6 (s,  $\text{H-C}_2$ )

ppm.

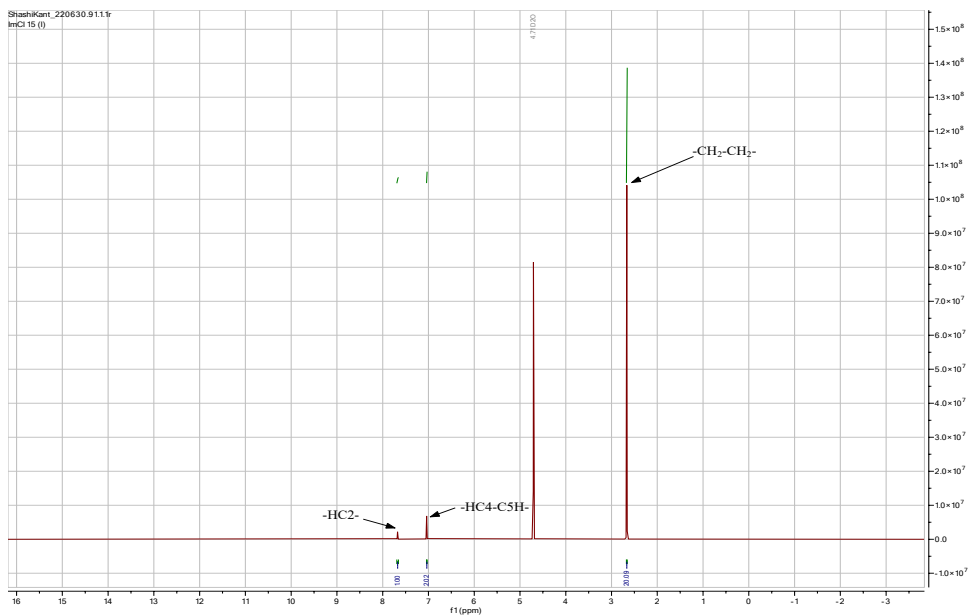


b)  $^{13}\text{C}$  NMR (400 MHz,  $\text{D}_2\text{O}$ , 25 °C): 42.0, 121.7 and 136.1 ppm.

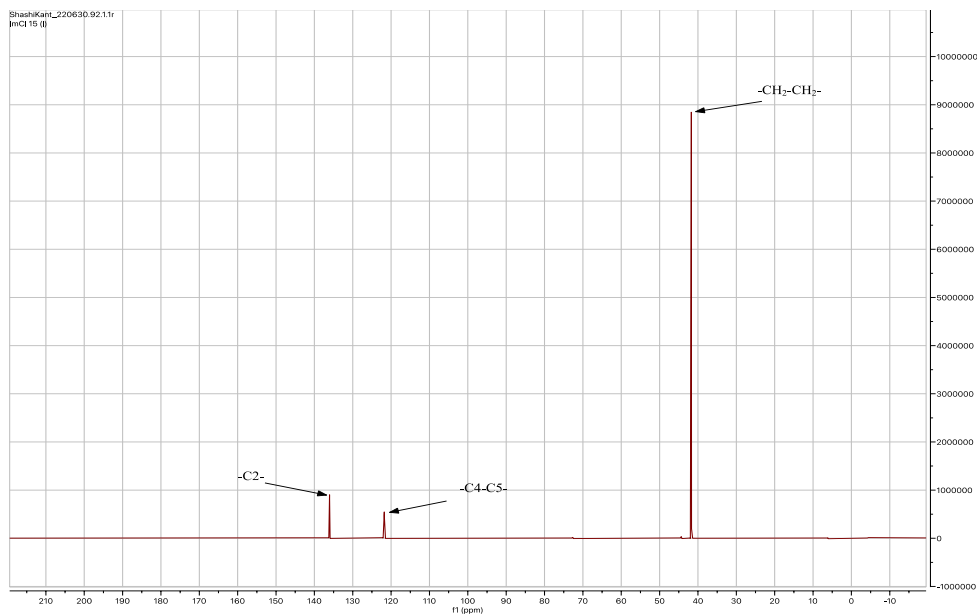


**[ImCl][EDA]=1:5**

a).  $^1\text{H NMR}$   $^1\text{H NMR}$  (400 MHz,  $\text{D}_2\text{O}$ , 25 °C):  $\delta\text{H}$  (ppm): 2.6 (s,  $\text{CH}_2\text{-NH}_2$  of EDA), 7.0 (s,  $\text{H-C}_4\text{-C}_5\text{-H}$ ), and 7.7 (s,  $\text{H-C}_2$ ) ppm.

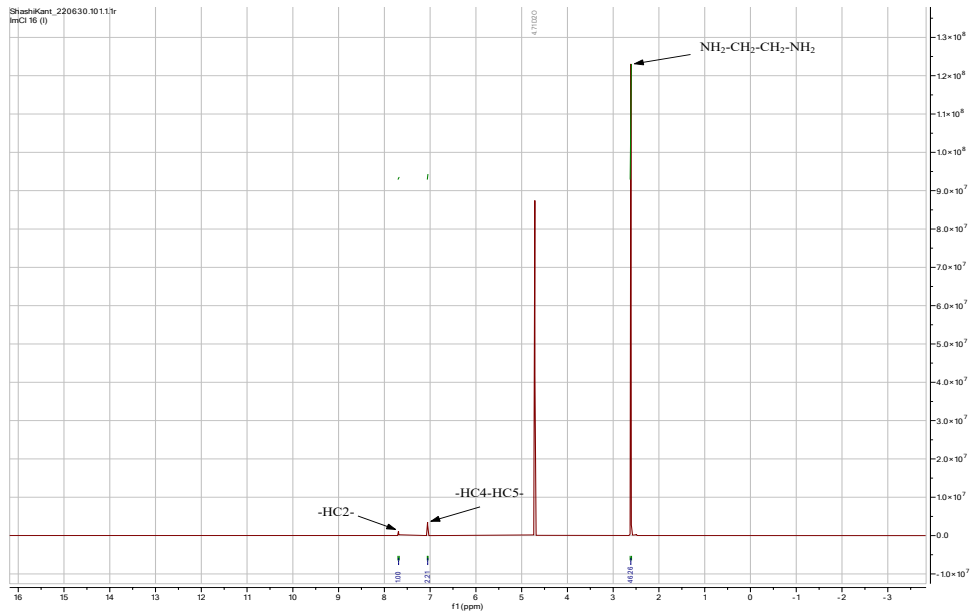


b).  $^{13}\text{C NMR}$   $^{13}\text{C NMR}$  (400 MHz,  $\text{D}_2\text{O}$ , 25 °C): 41.8.0, 121.7 and 135.9 ppm.

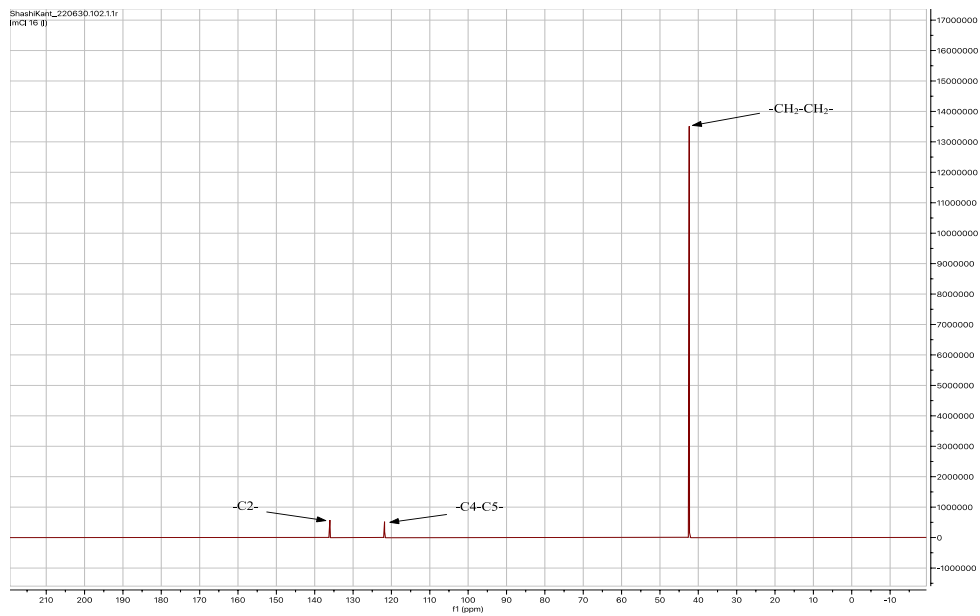


**[ImCl][EDA]=1:6**

a).  $^1\text{H NMR}$   $^1\text{H NMR}$  (400 MHz,  $\text{D}_2\text{O}$ , 25 °C):  $\delta\text{H}$  (ppm): 2.6(s,  $\text{CH}_2\text{-NH}_2$  of EDA), 7.0 (s, H-C<sub>4</sub>-C<sub>5</sub>-H), and 7.7 (s, H-C<sub>2</sub>) ppm.



b).  $^{13}\text{C NMR}$   $^{13}\text{C NMR}$  (400 MHz,  $\text{D}_2\text{O}$ , 25 °C): 42.3. 121.8 and 136.0 ppm.



### 3. DSC spectra of [ImCl][EDA]-based DESs

a).

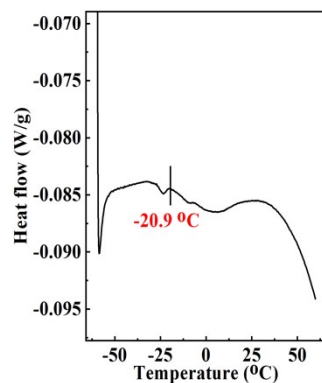


Fig. S1. DSC spectra of [ImCl][EDA]=1:4

b).

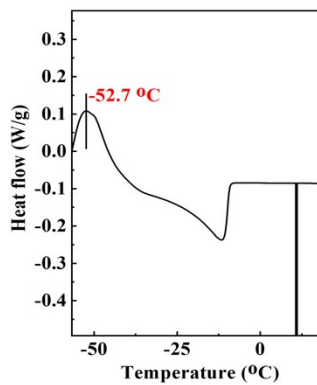


Fig. S2. DSC spectra of [ImCl][EDA]=1:5

c).

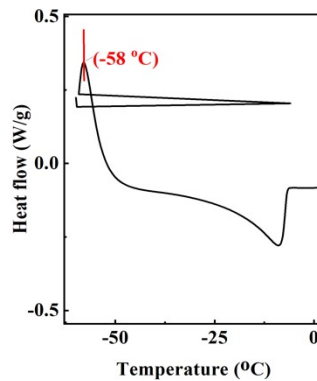


Fig. S3. DSC spectra of [ImCl][EDA]=1:6

#### **4. CO<sub>2</sub> uptake experiment and capture profile in 30% DES solutions**

The absorption experiments involved bubbling CO<sub>2</sub> gas into a vial containing 3 g of 30% DES solution at a 50 ml/min flow rate under inert conditions. The vial was weighed at regular intervals to measure the differential weight of absorbed CO<sub>2</sub>. This was used to calculate the weight percentage of absorbed CO<sub>2</sub> in the respective 30% DES solution. An electronic balance with an accuracy of  $\pm 0.1$  mg was used to weigh the vial.<sup>1</sup> Deionized water having a specific conductance of  $< 0.0055 \times 10^{-6}$  S.cm<sup>-1</sup> was used throughout the work.

## 5. DES recyclability experiment

The feasibility of recycling DESs was performed through the sequential absorption–desorption cycles with  $[\text{ImCl}][\text{EDA}]=1 : 4$  (ESI Fig. S4.). A 30 wt%  $[\text{Im}\cdot\text{Cl}][\text{EDA}]$  in ethylene glycol is taken as a reference solution for the recyclability test and the cut-off limit was set around 21 wt%.  $\text{CO}_2$  desorption in both cycles was achieved by heating the solution at 70 °C for 25 min under inert environment until complete desorption.

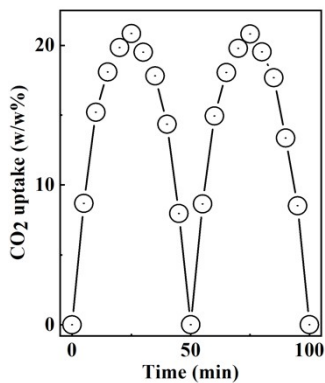


**Fig. S4.** Consecutive absorption–desorption cycles of 30 wt%  $[\text{ImCl}][\text{EDA}]=1 : 4$  in ethylene glycol. The absorption and desorption experiments were performed at room temperature and 70 °C, respectively.

## 6. DFT calculations

### Ion models and atomistic simulation methodology

For DFT calculations, an explicit solvent model with 15-20 water molecules, depending on reactant size, was adopted around the reactant structures, and the polarizable continuum model (PCM) was used at distances beyond the calculated solvation structure. Although water molecules did not participate in the reaction, they formed a hydrogen bond with reactant molecules (see ESI, Entry 6, Fig. S5-S8). The potential energy profile indicates four stationary points when a CO<sub>2</sub> molecule approaches the EDA molecule resulting in a zwitterion (ESI, Fig. S8). The zwitterion formed can undergo intermolecular or intramolecular H-abstraction or coordinate with an EDA molecule.

Quantum chemistry calculations were first performed to optimize molecular geometries of imidazolium (Im) cation and ethylenediamine (EDA) molecule using the Gaussian 16 package<sup>2</sup> with the Becke's three-parameter hybrid (B3LYP) functional and the 6-311++G(d, p) basis set. The atomic partial charges on these solvent molecules were computed by fitting to the molecular electrostatic potential at atomic centers with the Møller-Plesset second-order perturbation method and the correlation-consistent polarized valence cc-pVTZ(-f) basis set. The atomistic force field parameters for all ions and molecules were described in the AMBER format and taken from previous work.<sup>3</sup> The cross-interaction parameters between different atom types were obtained from the Lorentz-Berthelot combination rule.

Four modeling systems were constructed. The detailed simulation system compositions are listed in Table S1. Atomistic simulations of this modeling system were performed using the GROMACS package with cubic periodic boundary conditions.<sup>4</sup> The equations for the motion of

all atoms were integrated using a classic Verlet leapfrog integration algorithm with a time step of 1.0 fs. A cutoff radius of 1.6 nm was set for short-range van der Waals interactions and real-space electrostatic interactions. The particle-mesh Ewald (PME) summation method with an interpolation order of 5 and a Fourier grid spacing of 0.15 nm was employed to handle long-range electrostatic interactions in reciprocal space. All simulation systems were first energetically minimized using the steepest descent algorithm, and thereafter annealed gradually from 700 K to room temperature (300 K) within 10 ns. All annealed simulation systems were equilibrated in an isothermal-isobaric (NPT) ensemble for 20 ns of physical time maintained using a Nosé-Hoover thermostat and a Parrinello-Rahman barostat with time coupling constants of 0.5 and 0.2 ps, respectively, to control the temperature at 300 K and the pressure at 1 atm. Atomistic simulations were further performed in a canonical ensemble (NVT) for 80ns, and simulation trajectories were recorded at an interval of 100 fs for further structural and dynamical analysis.

**Table S1.**

|                     | System1                       | System2                       | System3                       |
|---------------------|-------------------------------|-------------------------------|-------------------------------|
|                     | ImCl:EDA=1:4                  | ImCl:EDA=1:5                  | ImCl:EDA=1:6                  |
|                     | ImCl-EDA:H <sub>2</sub> O=3:7 | ImCl-EDA:H <sub>2</sub> O=3:7 | ImCl-EDA:H <sub>2</sub> O=3:7 |
| ImCl                | 83                            | 70                            | 60                            |
| EDA                 | 332                           | 350                           | 360                           |
| H <sub>2</sub> O    | 3704                          | 3676                          | 3656                          |
| CO <sub>2</sub>     | 286                           | 322                           | 395                           |
| Total no. of atoms  | 16867                         | 16964                         | 17133                         |
| Simulation box size | (5.6768 nm) <sup>3</sup>      | (5.7307 nm) <sup>3</sup>      | (5.7651 nm) <sup>3</sup>      |

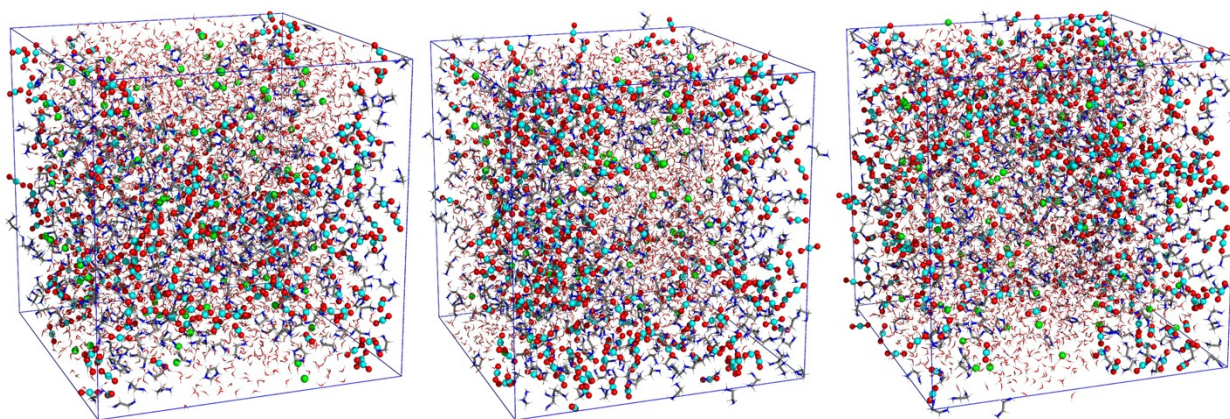


**Fig. S5.** Representative snapshots of four modeling systems obtained from extensive atomistic simulations.

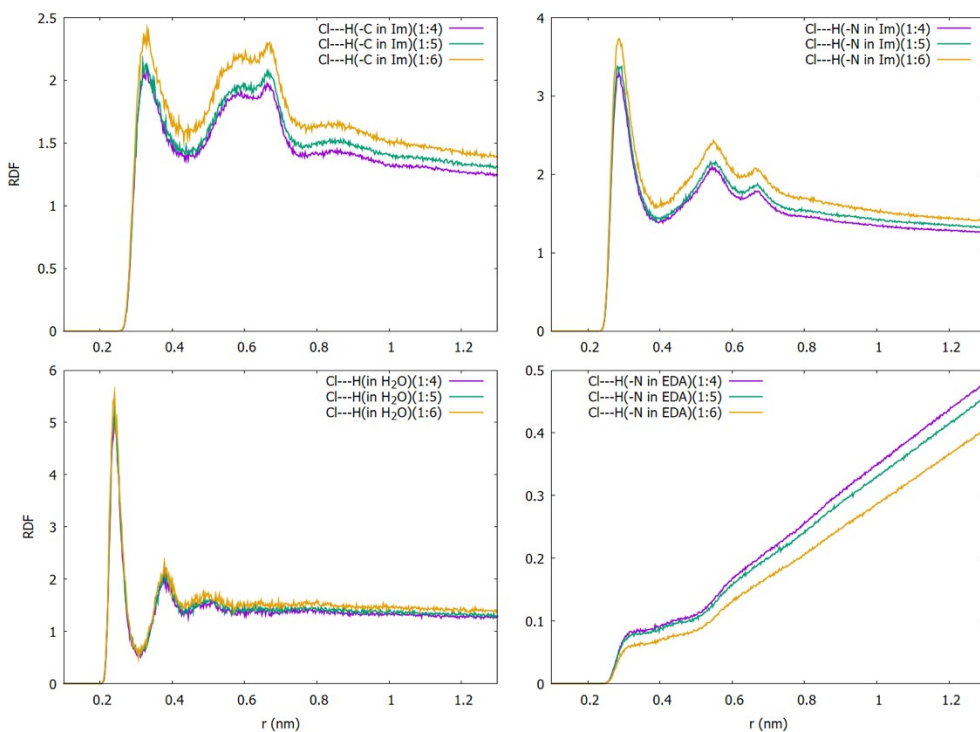


**Fig. S6.** Radial distribution functions of Cl anions with representative atoms in Im cations, EDA, and H<sub>2</sub>O molecules.

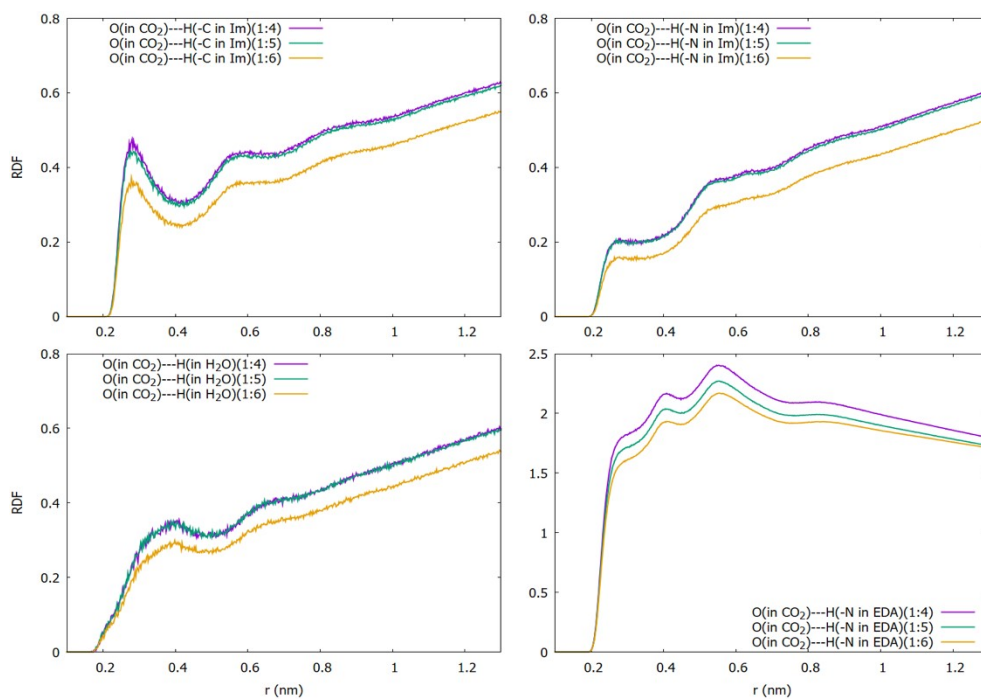


**Fig. S7.** Radial distribution functions of O atom in  $\text{CO}_2$  molecules with representative atoms in Im cations, EDA, and  $\text{H}_2\text{O}$  molecules.

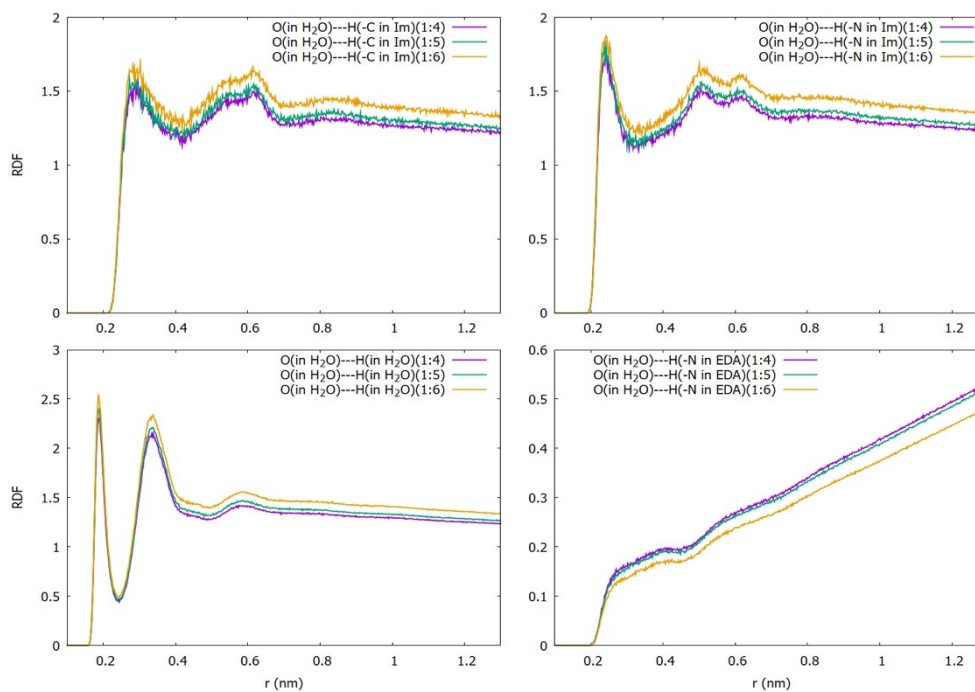


**Fig. S8.** Radial distribution functions of O atom in H<sub>2</sub>O molecules with representative atoms in Im cations, EDA, and H<sub>2</sub>O molecules.

## Results and Discussion

The scan of the potential energy profile for adding one CO<sub>2</sub> to the EDA molecule indicates four stationary points when approaching CO<sub>2</sub> to the EDA molecule. Starting from an infinite separation between the two reactants, the first minimum energy complex is found when the distance between the C atom in CO<sub>2</sub> and the N atom in amine is 2.75 Å. From the initial complex, the system evolves through the transition structure, where the relative energy is 3.52 kcal/mol and the C-N distance is 2.06 Å. In these two complexes, the CO<sub>2</sub> molecule is still linear and approaches the amine with the OCO axis almost perpendicular to the N-C bond of the amine. An additional transition structure with an OCO angle of approximately 143° was observed, and the OCO group and the C-N bond are nearly in the same plane. After this point, the relative energy falls to the value found for the formation of the zwitterion (6.05 kcal/mol), a minimum on the potential energy surface with an equilibrium C-N distance of 1.56 Å. An energy barrier of 11.07 kcal/mol was observed from the second transition structure to the zwitterion intermediate. These computational results align with that reported in the literature, which showed that carbamate formation follows a two-step mechanism with the zwitterion as an intermediate in 2-aminoethanol and 1,2-diaminoethane aqueous solution.<sup>5</sup>

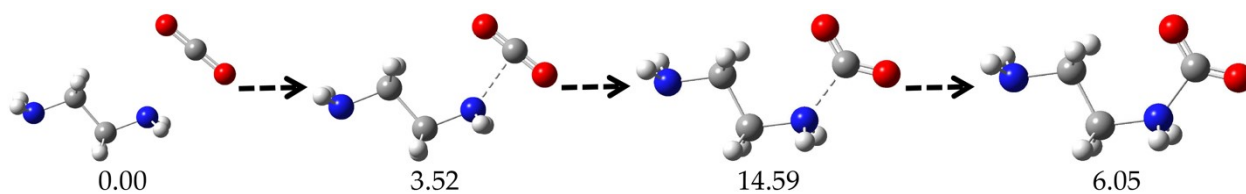


**Fig. S9.** Free-energy diagram for the reaction of one CO<sub>2</sub> with EDA molecule in an aqueous solution. The molecules around the target reactants are not shown for clarity issues

### 7. Depiction of pseudo-first-order rate constant ( $k$ )

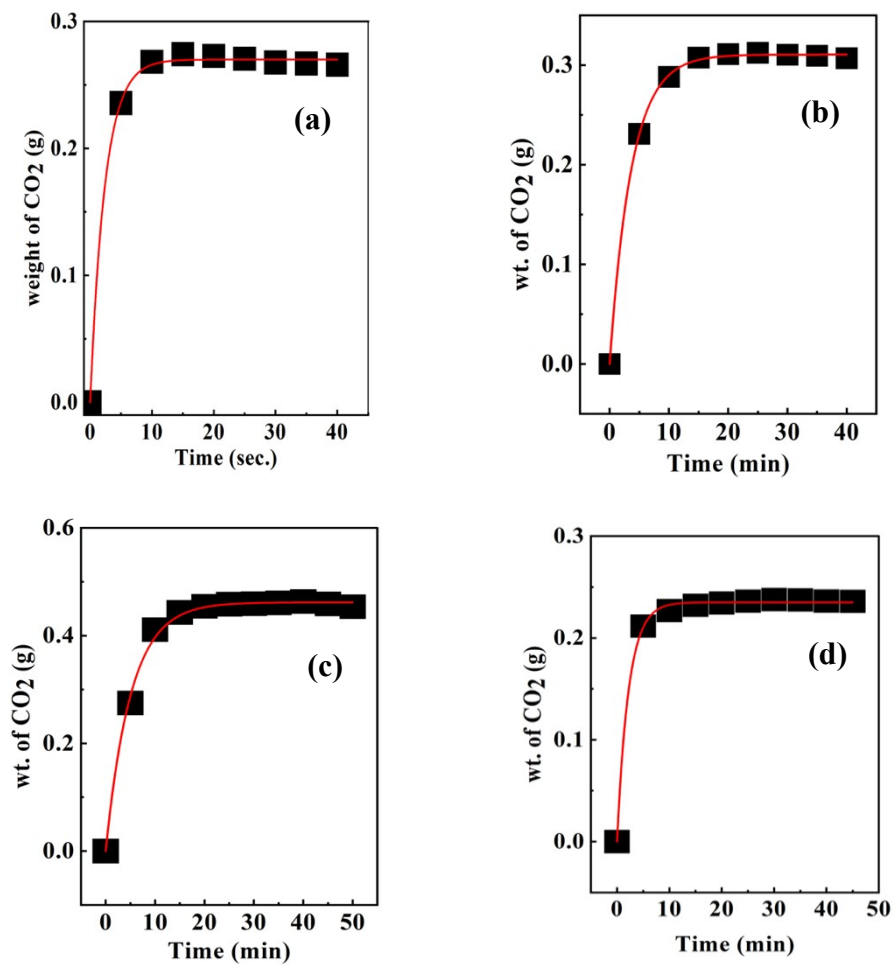


**Fig. S10.** A representative plot of weight of absorbed CO<sub>2</sub> against time in a DES to derive pseudo 1<sup>st</sup> order rate constant ( $k$ ).

**Table S2.** Table showing goodness of fit of the Box-Lucas equation in DESs

| Rate constant of solvents | Correlation coefficient (r) |
|---------------------------|-----------------------------|
| MEA                       | 0.99883                     |
| [ImCl][EDA]+1:4           | 0.99889                     |
| [ImCl][EDA]+1:5           | 0.99964                     |
| [ImCl][EDA]+1:6           | 0.99753                     |

**8. Depiction of enthalpy calculation from DSC spectrum**

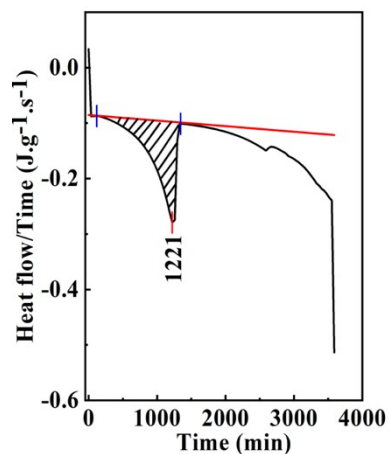


**Fig. S11.** A typical DSC spectrum for enthalpy calculation.

## 9. GC-MS calibration and typical GC-MS spectrum for decomposition calculations

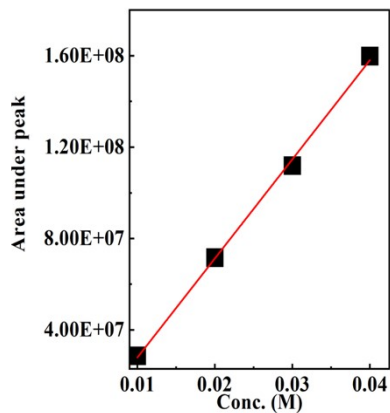


Fig. S12. GC-MS calibration curve for a typical DES.

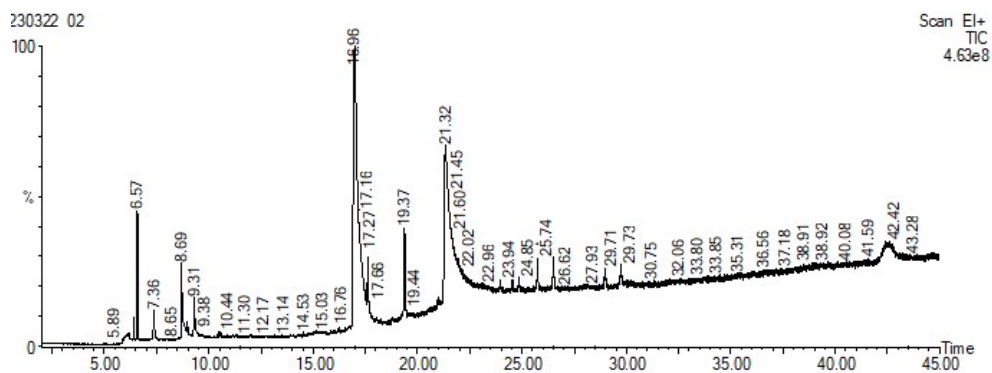
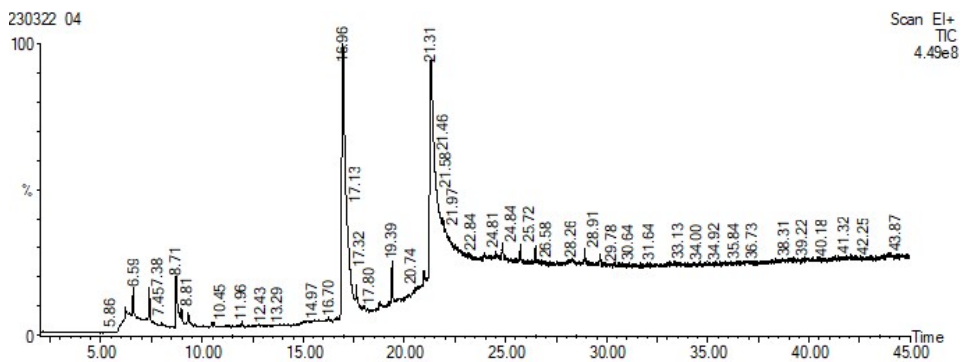
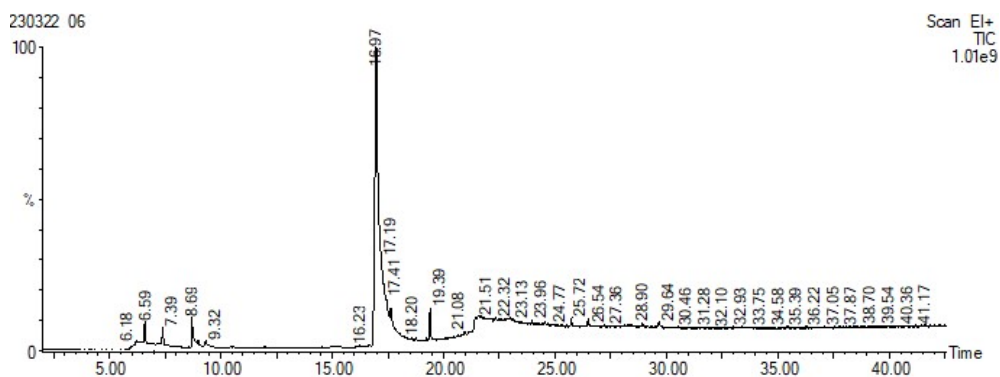


Fig. S13. GC-MS spectrum of thermally-pretreated (140 °C for two weeks) CO<sub>2</sub>-saturated 30% MEA in water.



**Fig. S14.** GC-MS spectrum of thermally-pretreated-(140 °C for two weeks) CO<sub>2</sub>-saturated 30% [ImCl][EDA]=1:4 in water.



**Fig.15.** GC-MS spectrum of thermally-pretreated-(140 °C for two weeks) CO<sub>2</sub>-saturated 30% [ImCl][EDA]=1:5 in water.

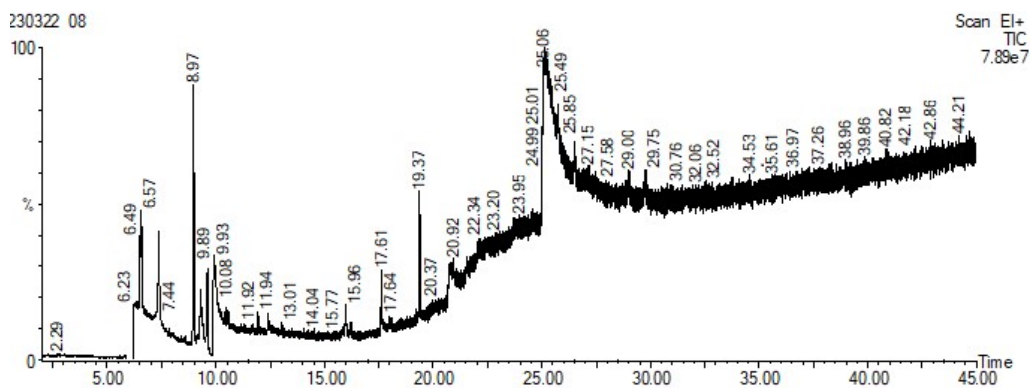


**Fig. S16.** GC-MS spectrum of thermally-pretreated (140 °C for two weeks) CO<sub>2</sub>-saturated 30% [ImCl][EDA]=1:6 in water.

## 10. GC-MS experimental details

The degradation study includes information on the extent of degradation, the mechanisms involved, the entities formed, and the associated risks. To investigate the thermal degradation of the 30% CO<sub>2</sub>-saturated [ImCl][EDA] solutions, a steel reactor equipped with the Teflon coating was used, and the solutions were heated at 140 °C for two weeks in a heating oven. Thereupon, the samples were analyzed using Gas Chromatography-Mass Spectroscopy (GC-MS). Thermal degradation analysis of 30% MEA and [ImCl][EDA]-based DES solutions was performed with the GC-MS instrument on a Clarus 690 MS coupled to Clarus SQ8 GC instrument (PerkinElmer, Waltham, MA, USA) equipped with a capillary column (Elite -FFAP; 30 m, 0.25 mm ID, 0.25 μm df, Cat. #N9316352; PerkinElmer). All the experiments were performed under the following conditions: the oven temperature for GC was kept at 50 °C for 0.5 min, then increased to 194 °C for 3.5 min at a rate of 30 °C/min, and finally ramped to 240 °C at 5 °C/min for 10 min. Helium (He) was used as a carrier gas in split mode (10:1) and 1 μL of the sample was injected at an injection port temperature of 250 °C. The MS transfer line temperature was adjusted to 250 °C with 170 °C source temperature. Mass spectra within 50 to 400 *m/z* were recorded at 3 scans/s with electron ionization at 70 eV.<sup>6</sup>

The percentage degradations of 30% MEA and DES solutions were determined by comparing the GC-MS spectrum of these solutions with respect to their calibration plots. A typical calibration plot is shown in Fig. S12.

## 11. Risk assessment of degradation products

**Table S3.** Risk assessment of degradation product of 30% MEA and [ImCl][EDA]-based DES solutions.

| Species   | Hazards   |
|---|---|
| <b>A)-Monoethanolamine (MEA)</b>                          |   |
| 1. 2-oxazolidinone  | low environmental <i>hazard</i>   |
| 2. N-(2-hydroxyethyl)ethylenediamine                      | Corrosive to tissue. Combustible, but may be difficult to ignite. Less dense than water. Vapors heavier than air  |
| 3. N-(2-hydroxyethyl)imidazolidinone                      | Not a hazardous substance or mixture according to Regulation (EC) No 1272/2008  |
| 4. N-(2-aminoethyl)-N'-(2-hydroxyethyl)imidazolidinone    | Not found/reported  |
| 5. N,N'-bis(2-hydroxyethyl)urea                           | Acute toxicity, Skin corrosion, Serious eye damage, Specific target organ toxicity, single exposure; Respiratory tract irritation, LDLo-9250 mg/k                           |
| <b>B)-[ImCl][EDA]-based Deep-Eutectic Solvents (DESs)</b> |   |
| 1. dichloromethane  | irritating to the eyes, skin, and respiratory tract, aspiration pneumonitis, affects central nervous system, blood, liver, heart, and lungs, carbon monoxide poisoning etc. |
| 2. dimethoxydimethylsilane                                | Flammable, eye irritation, respiratory irritation   |
| 3. 1H-pyrazole  | Acute oral toxicity, skin and eye irritation, respiratory irritation  |
| 4. hexamethylcyclotrisiloxane                             | Skin irritation, redness, swelling, production of vesicles, scaling and thickening of the skin  |
| 5. methoxyethane  | Irritation, flammable, thermally unstable, peroxidizable compound   |
| 6. 2-hydroxy-5-methylbenzophenone                         | Skin, eye, and respiratory tract irritation   |
| tertbutyldimethylether                                    | Skin and eye irritation, headache, dizziness, nausea, weakness, and lightheadedness. Affect liver and kidneys.  |

|   |   |
|---|---|
| 7. 1-chloro-2-nitroethane                                     | Combustible, redness, blue lips, dizziness, headache, nausea, shortness of breath, confusion, convulsion and unconsciousness.         |
| 8. 3-benzyloxy-2-fluoro-6-hydroxyphenylamine diisopropylamine | Not found/reported  |
| 9. 2,2-dimethoxybutane  | Coughing and shortness of breath, pulmonary edema, headache, nausea and vomiting.   |
| 10. androstane-11,17-dione                                    | Flammable, acute toxicity, skin and eye irritation, specific target organ toxicity.   |
| 11. triamcinolone acetonide                                   | Depression, puberty, miscarriage, liver problems, worsen polycystic ovary syndrome, and prostate cancer                               |
| 12. glycocholic acid  | burning, itching, irritation, stinging, redness, drying of the skin, acne, change of skin color, unwanted hair growth, tiny red bumps |
|   | None  |

## References.

<sup>1</sup> S. K. Shukla and J-P Mikkola, *Phys. Chem. Chem. Phys.*, 2018, **20**, 24591-24601.

<sup>2</sup> M. J. Frisch, G. W. Trucks, H. B. Schlegel, G. E. Scuseria, et. al. Gaussian, Inc., Wallingford CT, 2016.

<sup>3</sup> Z, Liu, S. Huang and W. Wang, *J. Phys. Chem. B*, 2004, **108**, 34, 12978–12989.

<sup>4</sup> M. J. Abraham, T. Murtola, R. Schulz, S. Páll, J. C. Smith, B. Hess and E. Lindahl, *SoftwareX*, 2015, **1–2**, 19-25.

<sup>5</sup> T. Davran-Candan, *J. Phys. Chem. A*, 2014, **118**, 25, 4582–4590.

<sup>6</sup> A. Patel, E. Krikigianni, U. Rova, P. Christakopoulos and Leonidas Matsakas, *J. Chem. Eng.*, 2022, **438**, 135529-135545.